DOI: 10.1002/cmdc.200700319

Towards an Integrated Description of Hydrogen Bonding and Dehydration: Decreasing False Positives in Virtual Screening with the HYDE Scoring Function

Ingo Reulecke,[a] Gudrun Lange,[b] Jürgen Albrecht,[b] Robert Klein,[b] and Matthias Rarey*[a]

We developed a new empirical scoring function, HYDE, for the evaluation of protein–ligand complexes. HYDE estimates binding free energy based on two terms for dehydration and hydrogen bonding only. The essential feature of this scoring function is the integrated use of log P-derived atomic increments for the prediction of free dehydration energy and hydrogen bonding energy. Taking the dehydration of atoms within the interface into account shows that some atoms contribute favorably to the overall score, while others contribute unfavorably. For instance, hydrogen bond functions are penalized if they are dehydrated unless they can overcompensate this loss by forming a hydrogen bond with excellent geometry. The main stabilizing contribution represents the removal of apolar groups from the water: the hydrophobic effect. Initial studies using the DUD dataset show that with HYDE, there is a significant decrease in false positives, a reasonable categorization of compounds as either non-binders, weak, medium or strong binders, and in particular, there is a generally applicable and thermodynamically sensible cutoff score below which there is a high likelihood that the compound is indeed a binder.

Introduction

Structure-based virtual screening and computer-aided lead optimization are well established in the pharmaceutical and agrochemical industries,[1] and complement other approaches such as combinatorial chemistry, fragment-based approaches, and high-throughput screening experiments. It has been shown that docking programs are usually successful in generating multiple poses that look sensible to a trained medicinal chemist and that include binding modes similar to that observed in the crystal structure.[2] Nevertheless, there is still much need for improvements in this field. Attempts to identify novel binders by virtual screening have not always been successful. Docking hit lists often include many interesting molecules that appear sensible. Most of these "sensible" compounds, however, will not bind to the target at reasonable concentrations.[3] In addition, recently published reviews emphasize that the prediction of binding affinity and the ranking of binders represents a major concern in drug design. Looking at scoring functions, it becomes clear that most scoring functions consist mainly of stabilizing terms, assessing discrete interactions and "hydrophobic contacts" only.[3–8] As a consequence, those compounds that form the maximal number of "interaction pairs" to the protein are scored highest. However, experimental observations suggest that there must be a reasonable number of destabilizing contributions. For instance, the destabilizing effect due to the dehydration of a hydrogen bond function buried in an apolar interface upon complex formation has been described but is often ignored.[9,10] However, recently published results that integrate dehydration descriptors suggest that the dehydration of polar groups urgently needs to be accounted for by a scoring function.[11]

Attempts to improve existing or to generate novel scoring functions have incorporated a variety of approaches.[8] For instance, the parameterization dataset of Surflex now includes artificial "negative data", which are supposed to include the unfavorable contribution to binding.[12] Because "non-binding" cannot be further experimentally quantified, correct calibration remains infeasible. Other empirical approaches incorporate explicit dehydration penalties into the scoring function. The ChemScore[13]-based GlideXP[14] function applies grid-based water desolvation energy terms. In addition, protein–ligand structural motifs leading to enhanced binding affinity are included: 1) hydrophobic enclosure where groups of lipophilic ligand atoms are enclosed on opposite faces by lipophilic protein atoms, 2) neutral–neutral single or correlated hydrogen bonds in a hydrophobically enclosed environment, and 3) five categories of charged–charged hydrogen bonds. The LigScore[15] functions consist of three distinct terms that describe the van der Waals interaction, the polar attraction between the ligand and protein, and the desolvation penalty attributed to the binding of the polar ligand atoms to the protein and vice versa. According to the HINT force field,[16] the contribution of a pair interaction is calculated from the log *P* value of the corresponding surface elements and is dependent on the distance between the interacting atoms. In addition, a logical function

[a] *I. Reulecke, Prof. Dr. M. Rarey*
Center for Bioinformatics, University of Hamburg
Bundesstraße 43, 20146 Hamburg (Germany)
Fax: (+49) 40-42838-7352
E-mail: rarey@zbh.uni-hamburg.de

[b] *Dr. G. Lange, J. Albrecht, Dr. R. Klein*
Scientific Computing, Bayer CropScience AG
Industriepark Hoechst, G836, 65926 Frankfurt am Main (Germany)

Supporting information for this article is available on the WWW under http://www.chemmedchem.org or from the author.

is included such that contacts between hydrophobic atoms and polar acid–base pairing are rewarded, whereas acid–acid or base–base contacts between polar atoms are penalized. X-Score[17] is an empirical scoring function in which $\log P$ parameters are used to account for the hydrophobic effect. X-Score sums up only the contributions of apolar atoms that are placed in an apolar environment using a switch function. The dehydration of polar atoms and of apolar atoms that do not point toward another apolar atom remains unconsidered.

We recently introduced a new concept in which the temperature-dependent fractions of saturated and unsaturated hydrogen bond functions within the water network are considered.[18] Based on this concept we derived novel terms for the dehydration of idealized polar and apolar functional groups and a simple explanation for the main characteristics of intermolecular interaction in aqueous solution, including the hydrophobic effect, dehydration penalties, and hydrogen bonding. Herein we introduce a scoring function, HYDE, which is based on these assumptions and uses $\log P_{o/w}$-derived atom parameters for the calculation of the dehydration free energy atom increments $\Delta G^i_{dehydration}$ and the contribution of the atoms i toward a hydrogen bond $\Delta G^i_{H\text{-}bond}$. The strengths and weaknesses of HYDE are demonstrated and discussed based on three enrichment studies using the database of useful decoys (DUD), which was recently published by the Shoichet research group.[19]

For a better understanding, some aspects of the concept that describes the interaction between idealized functional groups with the water network[18] are shortly summarized herein. Water can be characterized as a network with temperature-dependent fractions of saturated (f_{sat}) and unsaturated ($f_{unsat}=1-f_{sat}$) hydrogen bond functions. These fractions can be calculated by using a thermodynamic cycle. The f_{unsat} fraction ranges from roughly 0.11 close to the freezing point to 0.25 close to the boiling point of water. As a result of these unsatisfied hydrogen bond functions, the statistical energy contribution of a hydrogen bond between two water molecules within the water network $\varepsilon^{H_2O\cdots H_2O}$ is decreased by the factor f_{sat} relative to the hydrogen bond energy in the gas phase $\varepsilon_0^{H_2O\cdots H_2O}$.

$$\varepsilon^{H_2O\cdots H_2O} = f_{sat}\varepsilon_0^{H_2O\cdots H_2O} \quad (1)$$

Experiments show that polar functions which form hydrogen bonds to the water network with similar energy as those between water molecules, that is, $\varepsilon_0^{polar\cdots H_2O} \approx \varepsilon_0^{H_2O\cdots H_2O}$, integrate well into the water network,[20] and thus the hydrogen bond between an idealized polar function and the water network is decreased likewise:

$$\varepsilon^{polar\cdots H_2O} = f_{sat}\varepsilon_0^{polar\cdots H_2O} \quad (2)$$

Taking into account that for each dehydrated polar function one water function is released and two water hydrogen bond functions form a new hydrogen bond, the free energy for dehydrating an idealized polar function can be calculated as:

$$\begin{aligned} \Delta G_{dehydration} &= -f_{sat}\varepsilon_0^{polar\cdots H_2O} + \frac{1}{2}f_{sat}\varepsilon_0^{H_2O\cdots H_2O} \\ \Delta G_{dehydration} &\approx -\frac{1}{2}f_{sat}\varepsilon_0^{polar\cdots H_2O} \end{aligned} \quad (3)$$

Because the hydrophobic effect has been quantitatively described as the free dehydration enthalpy of an apolar function, we propose that the noncovalent contributions to intermolecular interactions in aqueous solutions, $\Delta G_{binding}$, can be calculated in a first approximation by considering only two main terms: a) the dehydration of the interacting molecular interfaces, $\Delta G_{dehydration}$, and b) the vacuum hydrogen bond energies between interacting hydrogen bond functions $\varepsilon^{polar1\cdots polar2}$. This approximation is only valid for complex structures in which repulsive steric interactions, both intra- and intermolecular, are small enough. It is acknowledged that the approach may be refined by adding a term that accounts for the entropy loss of molecules A and B upon complex formation.

$$\begin{aligned} \Delta G_{binding} &= \Delta G_{dehydration} + \sum_{i=1}^{n}\sum_{j=1}^{m}\varepsilon^{polar1\cdots polar2}\delta_{H-bond}(i,j) \\ \delta_{H-bond}(i,j) &= \begin{cases} 1 & \text{if H}-\text{bond between atom } i \text{ and } j \\ 0 & \text{otherwise} \end{cases} \end{aligned} \quad (4)$$

Here, $i=1\ldots n$ are the atoms of molecule A and $j=1\ldots m$ are the atoms of molecule B which together form the interface. The free energy of dehydration may be added directly to the interaction energies which leads to a hydrogen bonding term less than the hydrogen bond energy in the gas phase. Indeed, most scoring functions use a hydrogen bonding term that is decreased by a certain amount. However, it may be more straightforward and more intuitive to calculate the free dehydration energy independently because two processes that obey different physical principles are described.

Methods

According to the concept outlined above, the free energy of binding, $\Delta G_{binding}$, can be calculated as the sum over all atoms i contributing to the molecular interface:

$$\Delta G_{binding} = \sum_i \Delta G^i_{dehydration} + \Delta G^i_{H-bond} \quad (5)$$

Most functional groups do not belong to the idealized cases outlined above. Thus, a more general approach to estimate the hydrogen bond energies for all occurring functional groups was needed. Similarly, their dehydration cannot be calculated exactly by using the terms outlined for idealized functions. However, if either the free dehydration energy of a functional group or its hydrogen bond energy to water is available, Equation (3) can be used to estimate the missing value.

Prediction of free dehydration energy

HYDE uses atomic $\log P_{o/w}$ increments to estimate the dehydration contribution of each individual atom in the interface. The $\log P$ value of a compound is the logarithm of its partition coefficient $K_{o/w}$ between *n*-octanol and water. Assuming that the free desolvation energy of a molecule is smaller in octanol than that in water, the $\log P$ value can be used as a measure for the free dehydration energy of that molecule:

$$\Delta G_{\text{dehydration}} \approx -RT \ln K_{o/w} = -RT \frac{\log K_{o/w}}{\log e} = -2.3RT \log P \qquad (6)$$

for which R is the gas constant and T is the absolute temperature.

Various authors have approximated the $\log P$ value of a compound as a sum over individual atomic increments in order to predict $\log P$ values.[21–23] We also incorporated into the equation the atom's accessibility, which was previously shown to improve the results of $\log P$ prediction.[24,25] Summing up over all atoms i, the $\log P$ value can be approximated as:

$$\log P = \sum_i \frac{acc^i}{acc^k_{\text{mean}}} p \log P_k(i) \qquad (7)$$

for which acc^i is the calculated accessibility of an atom i in the molecule, acc^k_{mean} is the mean accessibility of an atom type k in the parameterization dataset, and $p \log P_k$ is the partial $\log P$ contribution of the atom type k. The accessibilities are calculated based on the solvent accessible surface (SAS) definition of Richards[26] and uses a spherical probe with a radius of 1.2 Å. Richards describes the SAS as the trace of the center of a spherical probe rolled over the van der Waals surface. In contrast to the non-directed interaction of a hydrophobic group with water, it is essential to take the directionality of the hydrogen bonds between polar groups and water molecules into account, and thus we included a weighting of the SAS of polar atoms. Only surface areas of an atom i that are located in the preferred direction of a hydrogen bond contribute toward the weighted solvent-accessible surface, $WSAS_i$. For practical reasons we divide $WSAS_i$ by the surface of a sphere of the corresponding size which leads to a dimensionless expression for the accessibility acc^i:

$$acc^i = \frac{WSAS_i}{4\pi(r_{\text{SAS}} + r^i_{\text{vdW}})} \qquad (8)$$

in which r_{SAS} is the probe radius, and r^i_{vdW} is the van der Waals radius of atom i. The exact calculation of $WSAS_i$ is illustrated in the computational section below.

For the $p\log P$ parameterization we used a selection of compounds from the Hansch and Leo collection of physicochemical properties,[27] which is provided as part of the PHYSPROP database by Syracuse.[28] HYDE uses $\log P$ increments to estimate the dehydration contribution of each atom separately, and therefore it is essential that the assigned $p\log P$ represents the physicochemical nature of the atom correctly. Ghose and Crippen[22] already pointed out that one of the major problems is the linear dependence between the atom types that are used to describe the various structural environments of atoms. In HYDE, only local influences are considered, that is, element, hybridization, number and type of outgoing bonds, and number of attached hydrogen atoms. By not discriminating further, a correlation with adjacent atom types is substantially circumvented, and the number of different atom types is kept low enough to avoid overfitting but still high enough to cope with the essential electrostatic differences. Charged species were excluded, as a molecule might possess different charged states in octanol and water. Thus, we decided not to differentiate between neutral and charged atom types. We chose a subset of 696 compounds with the constraint that a molecule must not contain more than one specific type of functional group. As Figure 1 shows, the multiple linear regression resulted in sensible $p\log P$ increments that can be reliably used for $\log P$ predictions. A listing of all atom types with their definition, $p\log P$ increments, and mean accessibilities (acc_{mean}) is given in Table 1.

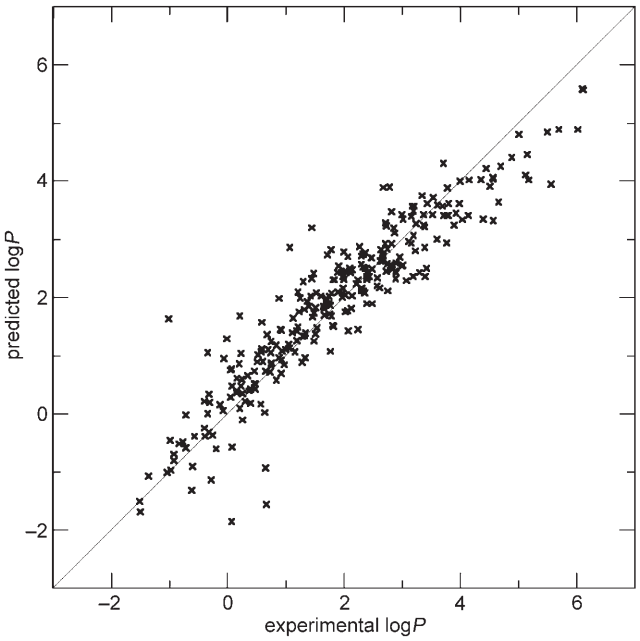

Figure 1. Experimental and predicted $\log P$ of the parameterization dataset (correlation coefficient: 0.93).

The dehydration energy of atom i can be calculated using its $p\log P$ increment and its accessibility in the complex acc_{complex} and in water acc_{free}:

$$\Delta G^i_{\text{dehydration}} = -2.3RT \frac{acc^i_{\text{free}} - acc^i_{\text{complex}}}{acc^i_{\text{mean}}} p \log P_i \qquad (9)$$

As apolar atoms obtain positive $p\log P$ values their dehydration contributes favorably, whereas polar atoms have a negative $p\log P$ value and thus their dehydration contributes unfavorably to the predicted binding free energy. Atoms with a

Table 1. Overview of HYDE atom types, *p*log*P*, and mean accessibility values.

Atom ID[a]	*p*log*P*	acc_{mean}	Comment(s)
Hydrogen	0.00	0.00	No contribution (definition)
C_sp_st_H0	0.00	0.18	Alkyne carbon
C_sp_st_H1	0.18	0.63	Alkyne carbon
C_sp2_aaa_H0	0.10	0.03	Aromatic carbon
C_sp2_saa_H0	0.00	0.02	Aromatic, no contribution
C_sp2_saa_H1	0.43	0.26	Aromatic carbon
C_sp2_ssd_H0	0.00	0.02	Alkene C, no contribution
C_sp2_ssd_H1	0.34	0.23	Alkene carbon
C_sp2_ssd_H2	0.77	0.56	Alkene carbon
C_sp3_ssss_H0	0.00	0.00	Alkane C, no contribution
C_sp3_ssss_H1	0.12	0.08	Alkane carbon
C_sp3_ssss_H2	0.48	0.24	Alkane carbon
C_sp3_ssss_H3	0.74	0.54	Alkane C, no contribution
Fluorine	0.30	0.36	Fluorine
Chlorine	0.56	0.40	Chlorine
Bromine	0.68	0.58	Bromine
Iodine	0.90	0.65	Iodine
N_sp_t_H0	−0.84	0.55	Nitrile nitrogen
N_sp2_aa_H0	−1.05	0.08	Aromatic nitrogen
N_sp2_saa_H0	0.00	0.04	Aromatic N, no contribution
N_sp2_saa_H1	−0.55	0.09	Aromatic nitrogen
N_sp2_snn_H0	0.00	0.11	Nitro
N_sp2_sss_H0	0.00	0.00	Planar amine nitrogen, no contribution
N_sp2_sss_H1	−1.15	0.06	Planar amine nitrogen
N_sp2_sss_H2	−0.94	0.15	Planar amine nitrogen
N_sp3_sss_H0	−1.43	0.03	Amine nitrogen
N_sp3_sss_H1	−1.72	0.10	Amine nitrogen
N_sp3_sss_H2	−1.31	0.22	Amine nitrogen
O_sp2_aa_H0	−0.63	0.14	Aromatic oxygen
O_sp2_d_H0	−0.80	0.17	Carbonyl oxygen
O_sp2_n_H0	0.00	0.38	Nitro oxygen
O_sp3_ss_H0_AA	−1.38	0.11	Ether (aliphatic/aliphatic) ester (aromatic)
O_sp3_ss_H0_Aa	−0.48	0.11	Ether (aromatic/aliphatic) ester (aliphatic)
O_sp3_ss_H0_aa	0.00	0.30	Ether (aromatic/aromatic)
O_sp3_ss_H1	−1.13	0.21	Hydroxy oxygen
O_sp3_ss_H2	−1.38	0.36	Water oxygen
C_sp_dd_H0	0.00	0.27	Allene carbon, insufficient information, set to zero
C_sp2_ggg_H0	0.10	0.10	Guanidinium carbon
Metal	−2.00	1.00	Metal ions
N_sp_st_H0	0.00	0.17	Nitrilium nitrogen
N_sp_st_H1	−0.84	0.10	Nitrilium nitrogen
N_sp2_sd_H0	−1.05	0.06	Imine nitrogen
N_sp2_sd_H1	−1.05	0.24	Imine nitrogen
N_sp2_ss_H0	−1.15	0.04	Deprotonated amine
N_sp2_ss_H1	−0.95	0.24	Deprotonated amine
N_sp2_ssd_H0	0.00	0.00	Iminium nitrogen
N_sp2_ssd_H1	−1.05	0.06	Iminium nitrogen
N_sp2_ssd_H2	−1.05	0.15	Iminium nitrogen
N_sp2_ssg_H0	0.00	0.02	Guanidinium nitrogen
N_sp2_ssg_H1	−1.15	0.05	Guanidinium nitrogen
N_sp2_ssg_H2	−0.94	0.13	Guanidinium nitrogen
N_sp2_ssm_H0	0.00	0.00	Amide nitrogen
N_sp2_ssm_H1	−1.15	0.04	Amide nitrogen
N_sp2_ssm_H2	−0.94	0.16	Amide nitrogen
N_sp3_ssss_H0	0.00	0.00	Ammonium nitrogen
N_sp3_ssss_H1	−1.43	0.01	Ammonium nitrogen
N_sp3_ssss_H2	−1.72	0.10	Ammonium nitrogen
N_sp3_ssss_H3	−1.31	0.21	Ammonium nitrogen
O_sp2_a_H0	−0.97	0.27	Carboxylate, derived from hydroxy and carbonyl
O_sp2_saa_H0	0.00	0.00	Charged aromatic oxygen
O_sp2_saa_H1	−0.54	0.11	Charged aromatic oxygen
O_sp3_s_H0	−1.13	0.37	Alcoholate
Phosphorus	0.00	0.00	No contribution
S_sp2_d_H0	0.00	0.60	No contribution
S_sp3_ss_H0	0.00	0.42	No contribution
S_sp3_ss_H1	0.00	0.64	No contribution
Silicon	0.00	0.00	No contribution
Sulfur	0.00	0.00	No contribution

[a] Coding of atom type identifiers: ⟨element⟩_⟨hybridization state⟩_⟨type of outgoing bonds⟩_⟨number of attached hydrogens⟩; bond types are: s = single, d = double, a = aromatic, m = amide, n = nitro.

mean accessibility in the uncomplexed state and which are completely buried upon complex formation contribute one *p*log*P* equivalent to the dehydration energy. Atoms that belong either to a protein or to a low-molecular-weight compound are treated identically. Note that due to the inclusion of the WSAS into the algorithm, the dehydration of polar atoms in narrow binding pockets is less expensive than the dehydration of solvent-exposed atoms, which is consistent with experimental observations.[29]

Prediction of hydrogen bond contribution

In the current FlexX interaction scheme, an ideal hydrogen bond always has the same contribution to the score, independent of the participating atom types. However, the use of identical hydrogen bond energies for all interacting pairs would lead to inconsistencies in HYDE because different atoms have different *p*log*P* values and are thus differently penalized for the dehydration. Therefore, we make use of Equation (3) in order to calculate the hydrogen bond energy, $\varepsilon_0^{polar\cdots H_2O}$, from the dehydration energy. The contribution of a polar atom toward a hydrogen bond is:

$$\Delta G^i_{H-bond} \approx \frac{1}{2}\varepsilon_0^{polar\cdots H_2O} \approx -\Delta G^i_{dehydration}/f_{sat} \quad (10)$$

ΔG^i_{H-bond} depends on the change of hydrogen bond saturation, sat^i, and the *p*log*P* value:

$$\Delta G^i_{H-bond} = \frac{2.3RT}{f_{sat}}\left(sat^i_{complex} - sat^i_{free}\right)p\log P_i \quad (11)$$

sat^i describes the degree of hydrogen bond saturation of atom i either in the complex ($sat_{complex}$) or in the unbound state (sat_{free}) and is calculated as:

$$sat^i = \sqrt{\sum_j f^{ij}_{dev}} \quad (12)$$

$f_{dev}(i,j)$ are the geometric penalty factors from the Böhm function,[30] which is explained in the computational section below; $f_{dev}(i,j)$ for a particular atom pair ij equals 1 if the hydrogen

bond has an ideal geometry, and 0 for large deviations from ideal values. The saturation sat^i of an atom i is calculated as the square root of the sum of the penalty factors over all corresponding atoms j in the proximity. We apply a square root term in order to avoid overrating of multiple hydrogen bonds. While only intramolecular hydrogen bonds are counted for the calculation of sat_{free}, interfacial hydrogen bonds are also considered for the calculation of $sat_{complex}$.

The geometry parameters used for the calculation of $f_{dev}(i,j)$ were readjusted to take into account the directionality of a hydrogen bond in a more stringent way and to reflect the experimental observations from small-molecule crystallographic data. Small-molecule data were used because their average coordinate error is much smaller than that in protein X-ray crystal structures, which have an average coordinate error of 0.2–0.4 Å at a resolution of 2.0 Å, and 0.5 Å at a resolution of 2.8 Å.[31] According to electrostatic[32] and quantum-mechanics-based models,[33] the hydrogen bond energy is already significantly decreased if the distance deviates by as little as 0.2 Å from the ideal value. This is also reflected in the distribution of hydrogen bond geometries observed in small-molecule crystallographic data. Interestingly, only after making the adjustments are the prediction of the hydrogen bond contributions and the balance between hydrogen bonds and hydrophobic effect in reasonable agreement with experimental observations.

In an alternative approach that also gives good results, the saturation change, $sat_{complex} - sat_{free}$, is calculated by considering the loss of accessibility due to the formation of a new hydrogen bond. Here too, the accessibilities are calculated by using the weighted solvent-accessible surface, and thus the contribution of hydrogen bonds with good geometry is larger than of those with poor geometry. In both approaches, the contribution toward a single hydrogen bond is always greater by the factor $1/f_{sat}$ than the penalty due to dehydration, which is roughly 1.2 at room temperature.

Docking and scoring of a protein–ligand interaction

As an application example, Figure 2 shows how HYDE scores the interaction between the biarylurea compound BIRB 796 and p38 MAP kinase (PDB code 1KV2[34]). To visualize the impact of a ligand atom, the score contributions from protein atoms are added to the contributions of the closest ligand atoms. The impact of an individual ligand atom is color-coded: green atoms contribute favorably, whereas red atoms contribute unfavorably to the overall binding energy. Figure 2 shows the superposition of the best-scored pose from docking and the original ligand structure.

Docking the compound using FlexX generates a pose that superimposes well with the crystal structure. The geometry of all hydrogen bonds is close to the ideal values, and thus the hydrogen bonds contribute fully ($f_{dev}(i,j) = 1$) to the total score. The calculated $\Delta G_{binding}$ value of -50 kJ mol^{-1} agrees well with the reported nanomolar binding affinity. The scoring of the original X-ray crystal structure shows that the polar atoms are similarly penalized for their dehydration, but the hydrogen bond energies are not fully realized due to small deviations

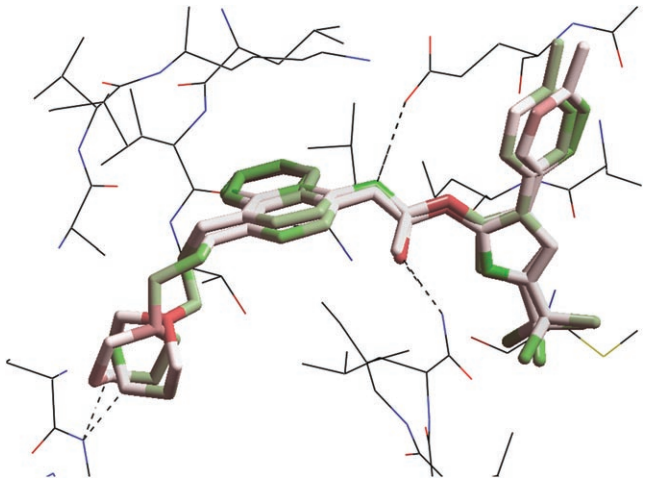

Figure 2. 3D representation of BIRB 796 bound to the allosteric site of p38 MAP kinase according to the crystal structure (PDB code 1KV2[34]) superimposed with the top-ranked docking pose. Atoms that contribute destabilization to the score are represented in red; atoms that contribute stabilization are displayed in green.

from the ideal geometry ($f_{dev}(i,j) = 0.63, 0.69, 0.72$). This results in a significantly smaller score of $\Delta G_{binding} = -36$ kJ mol^{-1}. The observed deviations are large enough to result in a decreased hydrogen bond energy. However, they are small enough to be within the average experimental error of protein crystal structures at this resolution (2.8 Å). Moreover, deviations of this size may very well relate to the geometric parameters used in the crystallographic refinement protocols. This shows that in the case of scoring crystal structures, a readjustment using the geometrical parameters of the scoring function is necessary prior to scoring.

Results

Various studies have compared the performance of docking tools and scoring functions in terms of identifying native-like binding poses, finding known binders of a specific target in a set of random compounds, and reproducing experimentally determined binding affinities.[2,35–39] We tested HYDE by using the database of useful decoys (DUD).[19] This recently published dataset consists of 40 different targets including published binders and decoy compounds. The decoy compounds were chosen such that they differ in topology from the binders but have similar physicochemical parameters in order to avoid an artificial enrichment due to parameters such as log P or the molecular weight of the compounds. Although the general idea to avoid bias due to physicochemical parameters is excellent, it should be pointed out that the approach to generate the decoys is very similar to the approach that medicinal chemists use to generate new compound classes. The decoy molecules are claimed to be non-binders, but there is no experimental confirmation for this. Therefore, it can be expected that some of them do not actually fall under the category 'non-binders', but represent potential new lead structures. This inconsistent categorization provides a possible explanation for

an enrichment lower than that of randomly selected libraries or libraries that contain only compounds with proven non-inhibition.

We docked the compound subsets into their specific targets using FlexX 2.1.0. The active site was defined by a radius of 8 Å around the heavy atoms of the native ligand. The protonation and orientation of polar and rotatable groups in the protein was done using standard program parameters. Protomers and tautomers were generated for all ligand compounds using PROTOPLEX™[40] and docked separately. The conformational energy of the individual poses was calculated using an augmented AMBER force field,[41] and poses with a conformational energy greater than 60 kJ mol^{-1} were rejected. The top-200 docking solutions for each compound were stored in mol2 format and subsequently rescored with HYDE. The highest-scoring representative of a compound was kept for the enrichment analysis.

The calculated enrichment plots for the 40 test cases showed that HYDE performs excellently on some test cases, but medium to even worse than random on others. In 13 of the test cases, HYDE achieved a significantly better result than the FlexX implementation[42] of the Böhm function. It performed comparably to the Böhm function in 15 cases and worse on 12 target proteins. Closer inspection of the docking results and particularly the ligand poses revealed several reasons for this result. The enrichment calculation reflects the whole process which includes target and library preparation, the pose generation, and finally the scoring. Thus, insufficient enrichment may also be due to issues that are not directly related to the scoring function. To analyze the quality of the process and the strength and weaknesses of HYDE, we show herein three examples for which either a good or a poor enrichment was achieved. The enrichment and score distribution plots for these three targets are shown in Figures 3 and 4. In addition, arrows mark the positions within the enrichments at which the HYDE score is −35, −30, or −25 kJ mol^{-1}. According to our experience the HYDE score for a standard-sized compound should be better than −25 to −30 kJ mol^{-1} in order to categorize a compound as a binder. Small fragments should have a score not worse than −15 to −25 kJ mol^{-1}. This agrees well with expected inhibition values. Details about the datasets and enrichment factors for both the HYDE and FlexX scoring functions are given in Table 2.

Table 2. HYDE enrichment factors of the selected datasets.[a]

Dataset	Number of ligands	Number of compounds	$EF_{0.5\%}$	$EF_{1\%}$	$EF_{5\%}$	$EF_{10\%}$
$ER_{agonist}$	67	2637	32.8 (0.0)	25.4 (6.0)	10.1 (3.9)	6.6 (2.2)
Thrombin	65	2249	21.5 (15.4)	20.0 (9.2)	8.3 (12.0)	5.2 (7.2)
p38 MAP kinase	255	8642	0.0 (2.4)	0.4 (2.4)	1.0 (2.3)	1.2 (2.5)
p38 MAP BU subset	44	8642[b]	0.0 (0.0)	2.3 (0.0)	3.0 (1.4)	6.8 (1.1)

[a] The numbers show HYDE enrichment factors of discrete percentages of the rank-ordered datasets; FlexX results are given in brackets. [b] Note that the ratio of decoys to actives is sixfold higher in this example.

Estrogen receptor

The active site of the estrogen receptor (PDB code 1L2I[43]) is a deeply buried and hydrophobic cave in the protein interior with two hydrogen bond acceptor groups located on opposite surfaces. Typical binders have either steroid-like topology or are aromatic systems with hydrogen bond functions separated by approximately 12 Å. Visual inspection of the poses shows that FlexX generates the correct pose for the ligand in 1L2I and sensible poses for most binders as well. HYDE scores the original ligand and most of the 67 binders reasonably well, and the 2570 decoys much worse (Figure 4a). Figure 5a shows the rating of the original ligand of 1L2I. Its HYDE score of −43 kJ mol^{-1} agrees well with the reported inhibition of less than 10 nM. There is a significant contribution corresponding

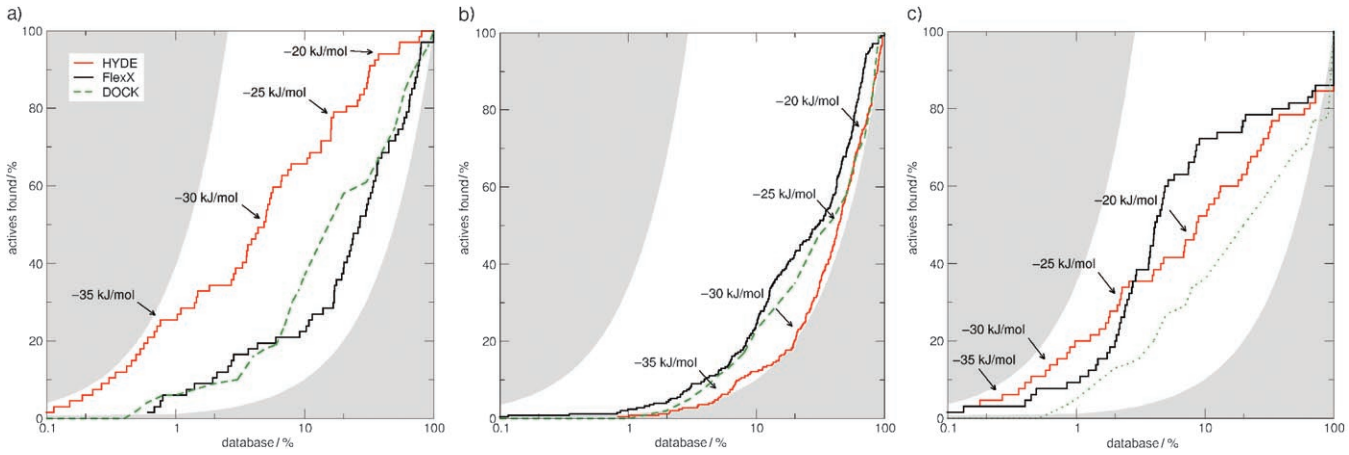

Figure 3. Enrichment plots for a) estrogen receptor, b) p38 MAP kinase, and c) thrombin. HYDE results are drawn in red, FlexX results in black. Arrows indicate the position within the enrichments at which the HYDE score is −35, −30, −25, and −20 kJ mol^{-1}. The dashed green line represents DOCK results which were extracted from Huang et al.[19]

to $-22\,kJ\,mol^{-1}$ due to the burial of apolar ligand atoms and of $-17\,kJ\,mol^{-1}$ due to the burial of apolar protein atoms. The hydrogen bonds contribute favorably by between -1 and $-5\,kJ\,mol^{-1}$ each. Similar contributions and interactions were observed for most binders. In addition to a substantial contribution due to the hydrophobic effect, the required hydrogen bonds are made with good geometry and thus contribute favorably to the overall score. Thirteen binders had a HYDE score of less than $-25\,kJ\,mol^{-1}$. No reasonable pose was identified for two binders which may be due to the fact that the protein would need to change its conformation, or through failure of FlexX to generate the correct pose. Most decoys, however, are not compatible with the binding site and are either strongly penalized for the burial of polar atoms in the protein–ligand interface or give rise to a substantially lower hydrophobic effect upon ligand binding. In contrast, the intrinsic scoring function of FlexX does not distinguish well between the binders and decoys (Figure 4b). An inspection of those compounds that are highly ranked by FlexX suggests that incorrect poses can still achieve a relatively high score value because the Böhm function does not take the unfavorable dehydration of polar atoms into account. As an example, Figure 5b shows the rating of decoy ZINC03977652 according to the FlexX score. Its total score of $-33\,kJ\,mol^{-1}$ results from the contributions of several hydrogen bonds and "hydrophobic interactions". However, the dehydration of the nitrogen atoms is ignored, and they contribute favorably to the score. In contrast, HYDE takes the unfavorable dehydration of the nitrogen atoms into account and as a consequence, categorizes this decoy as nonbinding ($-12\,kJ\,mol^{-1}$). This is indicated in Figure 5c by the unfavorable red coloring of the nitrogen atoms.

To analyze the performance of HYDE on a random library, we added 2500 randomly selected compounds from the Bayer CropScience in-house library to the 67 binders. The enrichment and the normalized score distribution show an even clearer separation between binders and randomly chosen molecules for this case relative to that of the calculations using the decoys (Figure 5d,e). In combination with our experience that scores better than -25 to $-30\,kJ\,mol^{-1}$ are reasonable for binders, we suspected that the decoy-generation process has created some weak leads, and thus some additional binders may be hidden in the decoy subset. Indeed, we suggest, for instance, that the decoy compounds ZINC01666289 ($-36\,kJ\,mol^{-1}$), ZINC00007254 ($-34\,kJ\,mol^{-1}$), ZINC00392984 ($-34\,kJ\,mol^{-1}$), ZINC00184724 ($-38\,kJ\,mol^{-1}$), and ZINC03950321 ($-31\,kJ\,mol^{-1}$) are weak binders. As an example, Figure 5f shows ZINC01666289 color coded according to the individual atom score contributions that were calculated with

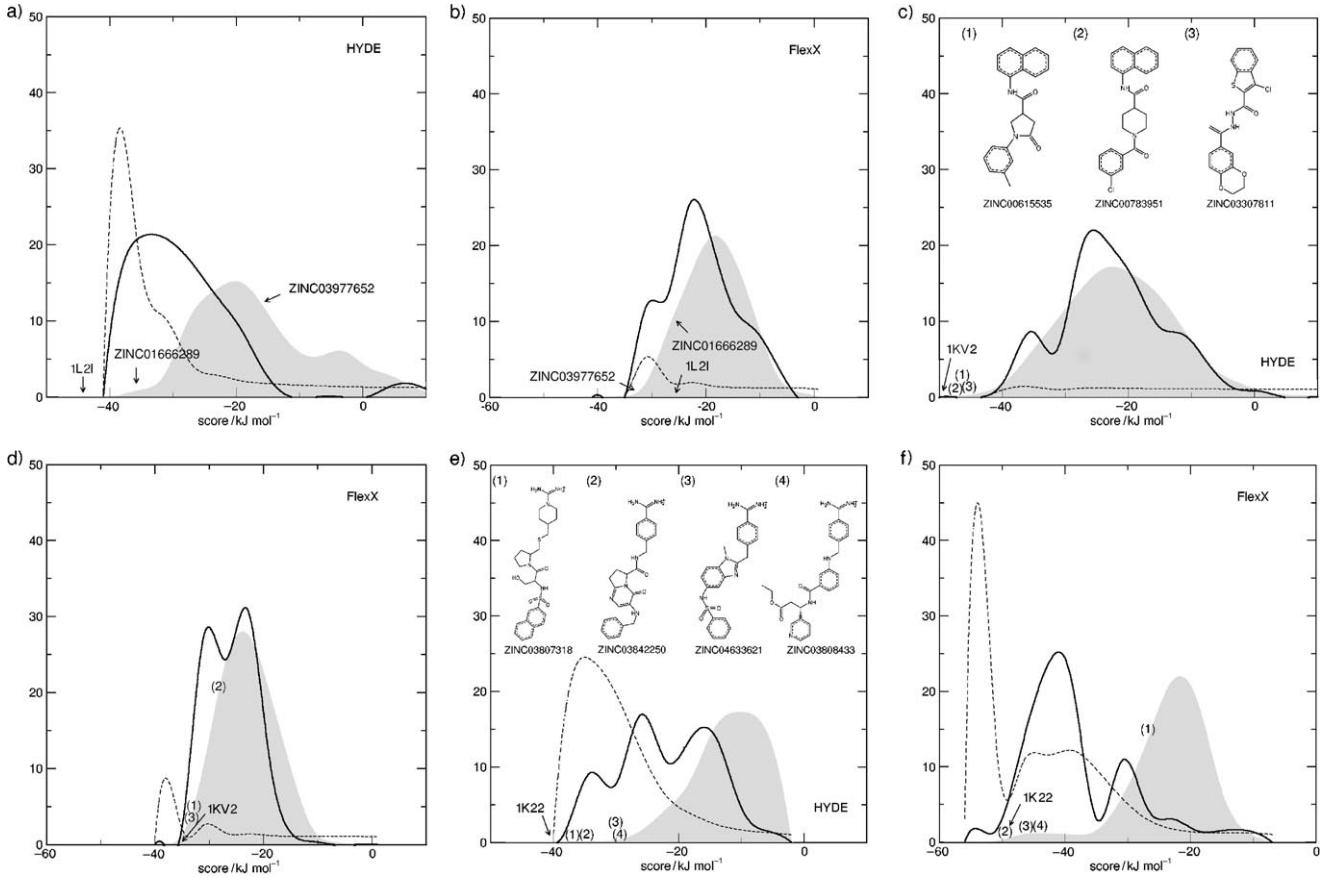

Figure 4. Normalized percentage of binders (bold lines) and decoys (gray areas) as a function of the score for a),b) the estrogen receptor, and c),d) p38 MAP kinase, and e),f) thrombin. The graphs were calculated using either the results of the HYDE (a,c,e) or the FlexX (b,d,f) scoring function. Dashed lines represent the enrichment factor as a function of the respective score. Arrows indicate the position of the score of the inhibitor in the original crystal structure and selected binders and decoys. These plots show only those compounds for which a solution with a conformational energy below $-60\,kJ\,mol^{-1}$ was found.

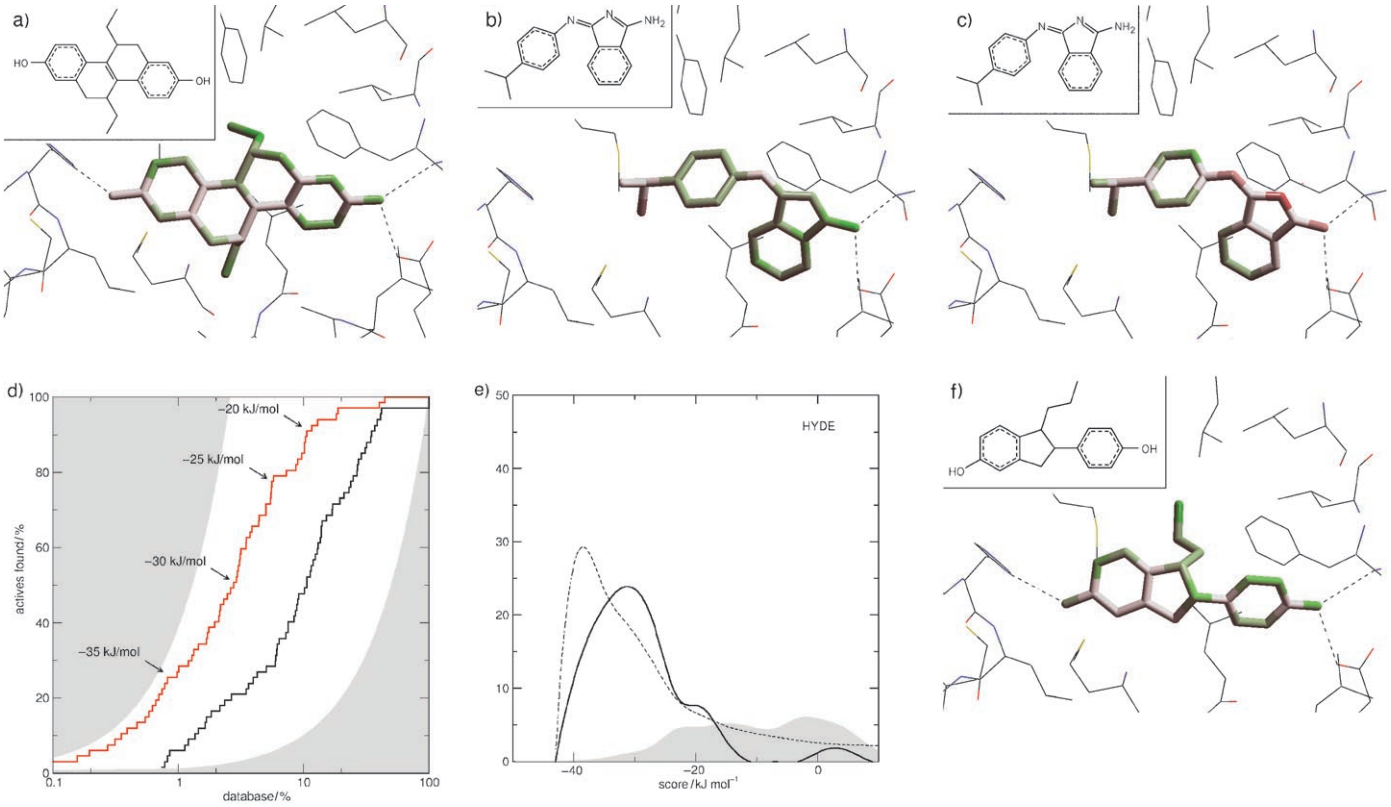

Figure 5. Selected examples for the estrogen receptor results: a) HYDE rating of original inhibitor 1L2I, b) FlexX rating of decoy ZINC03977652, c) HYDE rating of ZINC03977652, d) enrichment plot using a random compound library as non-binders, e) corresponding HYDE score contribution, and f) HYDE rating of putative binder ZINC01666289. Atoms contributing favorably according to the respective score are shown in green, and those contributing unfavorably are shown in red.

HYDE. Most of the important features of the original inhibitor in 1L2I, such as the hydrogen bonds and the burial of one of the ethyl groups, are conserved. Detailed analysis also suggests that the lower score of ZINC01666289 ($-36\ kJ\,mol^{-1}$) relative to the original ligand ($-43\ kJ\,mol^{-1}$) may be due to the lack of the second ethyl group, which contributes approximately $-5\ kJ\,mol^{-1}$ in the case of the original ligand. The presence of these presumably micromolar binding inhibitors within the decoy compounds explains the shoulder in the decoy enrichment around the score of $-32\ kJ\,mol^{-1}$ and thus why the enrichment above this value is significantly worse than the enrichment with a randomly selected compound library. Here, the likelihood is much greater that the compounds are indeed non-binders. Above $-20\ kJ\,mol^{-1}$ it can be assumed that these compounds are either non-binders or that no sensible pose has been generated.

p38 MAP kinase

Kinases are popular targets in pharmaceutical research, as they are involved in many relevant biochemical signaling pathways. Thus, the p38 MAP kinase subset of 440 binders and 8387 decoys in the DUD set is second-largest in size and contains up to tenfold more compounds than most of the other target protein subsets. Surprisingly, we could not achieve any enrichment of the binders in the dataset when we screened the binders against the kinase structure from the DUD database. Crystal structures have provided evidence that most kinase inhibitors bind to the hinge region of the ATP binding pocket. However, the protein structure provided with the DUD dataset (PDB code 1KV2[34]) represents a complex between a kinase and a biarylurea located in an allosteric binding site. Binding of this compound requires a large conformational change (Figure 6a), and as a result, inhibitors that bind to the hinge region of the ATP binding pocket do not fit into this particular protein conformation.[34]

An inspection of the binder dataset revealed that it contains tautomers and protomers for some compounds, while for others this was not the case. After careful revision, the number of binders was decreased from 440 to 256 compounds.[1] All reasonable tautomers and protomers were included as described above. A closer analysis of the compounds showed that many of the provided binders belong to compound classes for which crystallographic studies have shown that they occupy the ATP binding pocket. For instance, a significant portion of the compounds, 189 in total, has the triarylpyrrole topology of typical kinase inhibitors (TA), which bind according to their crystal structures to the hinge region of the ATP binding pocket.[44,45] For other compounds such as the 22 pyrrolo-

[1] *The revised ligand datasets are available directly from the authors upon request.*

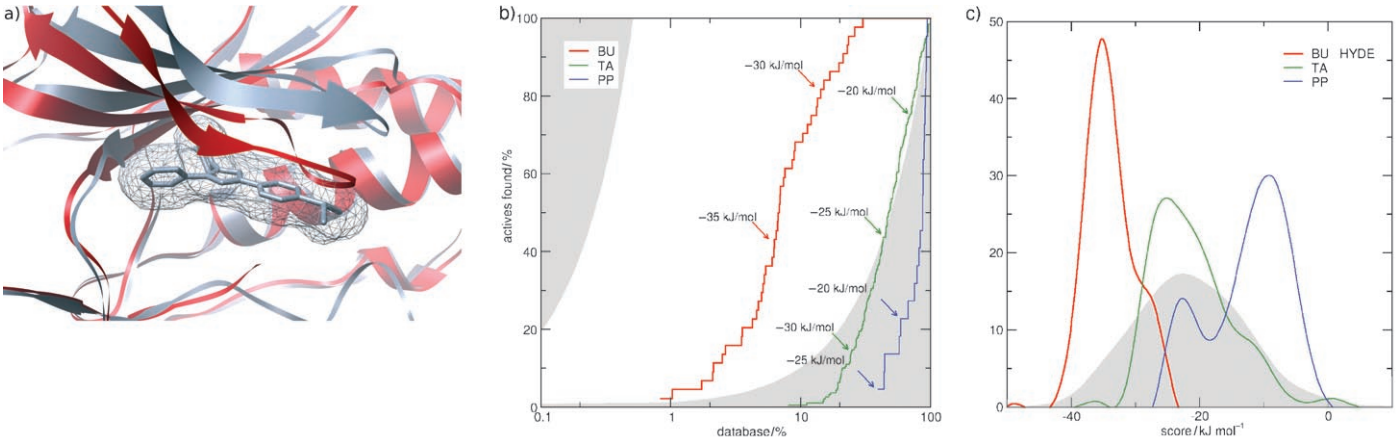

Figure 6. a) Superposition of p38 MAP kinase structures 1KV2[34] (red) and 1A9U[62] (gray). The triarylpyrrole compound associated with the ATP binding site of 1A9U is represented in gray sticks. b) Enrichment plot for individual subsets of the p38 MAP kinase binder dataset and c) the corresponding HYDE score distributions. The biarylurea compounds (BU) are represented by the red lines, the triarylpyrrole subset (TA) is shown in green, and the pyrrolopyrimidines (PP) are drawn in blue.

pyridines (PP), there is crystallographic evidence that they bind in the ATP binding site.[46] Only for the 44 compounds that belong to the biarylurea class (BU) is there reasonable evidence that they should be found using this particular protein structure. Thus, the disappointing enrichment observed in Figure 3b clearly results from an unsuitable combination of 'binders' and binding pocket. In order to challenge our scoring function, we repeated the enrichment calculations in three scenarios assuming that 1) only the 44 BUs are binders, 2) only the 22 PPs are binders, and 3) only the TAs are binders. In scenario 1, we expect a reasonable enrichment, whereas in scenario 2, we expect that the scoring function would give rise to an enrichment that is substantially worse than that of a random selection. As Figure 6b shows, there is indeed a considerable enrichment in the case of the BUs, whereas the enrichment of the TAs shows random-like behavior, and the enrichment of the PPs is much less than random. In particular, all 44 BUs are scored better than $-25\ kJ\,mol^{-1}$. In contrast, the PPs were scored very low by HYDE, with only one compound having a score better than $-25\ kJ\,mol^{-1}$ (Figure 6c). Here, the significant unfavorable contributions due to the dehydration of the polar ligand atoms are not outweighed by favorable contributions due to the hydrophobic effect. The TA compounds fall into a different category. Figure 6c shows that the best-scored compounds have a score typical for a "binder", whereas most of the compounds score between -25 and $-15\ kJ\,mol^{-1}$. A closer analysis shows that most of the favorable contributions are due to the significant hydrophobic effect, while only few or no hydrogen bonds are made for the highly ranked TAs. Thus, we propose that some of the better-scored compounds may indeed bind weakly into the allosteric binding pocket, but may lack specificity due to the absence of hydrogen bonds.

There appear to be further reasons for the relatively poor enrichment. Most of the best-rated decoy compounds belong to a limited number of structural classes. A literature analysis revealed that many of these compounds belong, or are closely related, to structural classes that are patented as kinase inhibitors.[47,48] These include ZINC00615535, ZINC01072327, ZINC00788124, ZINC00290115, ZINC00615522, ZINC00432687, ZINC00843792, ZINC01103953, ZINC00035049, ZINC03307811, ZINC01780257, ZINC02748340, ZINC03296097, ZINC02751904, ZINC00124860, ZINC03855198, ZINC03284746, ZINC03852818, ZINC02761165, and ZINC02754843. A sequence analysis of the binding site showed that the amino acids directed toward the allosteric binding site are highly conserved, suggesting that compounds binding into the p38 MAP kinase pocket should also be able to bind to other kinases. Thus, we conclude that there is a good chance that these decoys are categorized correctly as binders to p38 MAP kinase. This shows that for case of p38 MAP kinase as well, HYDE is able to recognize different classes of binders, to distinguish between binders and non-binders, and even to identify "unknown" binders in a library under investigation.

Thrombin

As a typical serine protease, thrombin is characterized by the catalytic serine residue, a charged aspartate at the bottom of the otherwise hydrophobic S1 pocket, and two further hydrophobic sub-pockets that are separated from each other by a β-sheet structure. In particular, there is an intricate hydrogen bond network between the ligand and the active site involving Asp 189, Gly 219, and a conserved water molecule. Closer inspection of the first docking attempts using the provided PDB file 1BA8[49] showed that neither the original inhibitor nor benzamidine was correctly placed within the active site using FlexX. This may be due to the fact that the inhibitor in 1BA8 is covalently linked to the protein, thereby causing a distortion in the active site such that the intricate hydrogen bonding network with the ligand cannot be realized with sufficiently good geometry. FlexX generated only poses with the amidine group interacting with other charged amino acids such as Glu 217. We therefore attempted to dock the provided 72 binders and

2184 decoys into an alternative thrombin structure, PDB code 1K22,[50] which seemed more suitable. The inhibitor of 1K22 and the benzamidine were correctly placed. The inhibitor had a score of $-42\ kJ\,mol^{-1}$, which agrees reasonably well with the reported $\Delta G_{binding}$ value of $-48\ kJ\,mol^{-1}$.[50] The score of $-18\ kJ\,mol^{-1}$ for benzamidine correctly suggests a millimolar to weak micromolar binder.

However, even with this alternative protein structure, the enrichment (Figure 3c) was not satisfying, and there was no clear separation between binders and decoys (Figure 4e). A subsequent closer inspection of the docking poses of the provided binder revealed that some compounds are placed correctly and scored better than $-25\ kJ\,mol^{-1}$. However, the 13 amidinobenzimidazoles such as ZINC03834109 had an unexpected low score. This was due to the fact that in the original DUD set, the amidine groups were stored with the wrong structure as geminal diamines and that they bind in the presence of zinc in the interface which was not included in the docking procedure.[51] The amidine groups were corrected and tautomers were omitted thereby decreasing the number of binders to 65. The assignment of "binder" ZINC03834158 as non-binding based on the HYDE score is correct, because this inhibitor binds irreversibly to the active site serine after ring opening has taken place.[52] In the case of binder ZINC03831937 ($-19\ kJ\,mol^{-1}$), a hydrogen bond contribution of approximately $-10\ kJ\,mol^{-1}$ is not included in the score because the hydroxy group hydrogen atom of Ser195 points in the wrong direction, and rotation of hydroxy groups on protein side chains is not a standard feature of FlexX. Furthermore, some of the standard amidines were not correctly placed, which may be due to the placement procedure of FlexX or due to protein flexibility. A second reason for the worse than expected enrichment is that some decoys scored surprisingly high. A subsequent literature analysis showed that most of the 30 decoys that score better than $-25\ kJ\,mol^{-1}$ either belong to known thrombin inhibitor classes or are even disclosed as thrombin inhibitors.[53–56] The 10 highest-scored decoys include thrombin inhibitors ZINC03807318 ($-37\ kJ\,mol^{-1}$), ZINC03807319 ($-33\ kJ\,mol^{-1}$), ZINC03842250 ($-35\ kJ\,mol^{-1}$), ZINC03838231 ($-31\ kJ\,mol^{-1}$), ZINC04633621 ($-30\ kJ\,mol^{-1}$), and ZINC03808433 ($-30\ kJ\,mol^{-1}$). Figure 7a shows the docked inhibitor of 1K22, and Figure 7b, the best-scored pose of decoy ZINC03842250 as an example. Clearly, similar interactions including the same hydrogen bond network and burial of hydrophobic substituents into apolar protein pockets have been identified for the binder in the crystal structure and ZINC03842250. Thus, in the case of thrombin, the unsatisfying enrichments can be explained by a) the incorrect placement of some binders by FlexX which must therefore be considered as non-binders under these conditions, and b) the fact that many of the best-scoring decoys are incorrectly categorized and are indeed binders.

Discussion

Scoring functions for the evaluation of protein–ligand interactions are used for several different tasks. As Leach et al. pointed out, they are used, among other things, to: a) predict a pose of a known binder in the absence of a crystal structure, b) identify novel binders by virtual screening of libraries, and c) rank known binders according to their affinity.[3] There is a general feeling that most predicted poses are quite sensible and "native-like" using currently available scoring functions. However, according to Leach, one cannot be sure whether the correct pose has been generated by the pose generator or whether the correct pose has the best score. Thus, in the absence of a crystal structure, some doubts remain whether the predicted pose should be used for further analysis and predictions. Most publicly available scoring functions seem to be able to identify unreasonable candidates, but fail to consider some important features, giving rise to a large number of false positives. Moreover, the correct ranking of binders remains a challenge.[3]

Enrichment calculations based on an active/inactive classification are therefore widely used to evaluate the quality of scoring functions. Enrichment calculations show the ranking of known binders according to their score ideally in comparison with the ranking of compounds that are known not to bind to the target protein. Studies have shown that most available scoring functions do not seem to produce comparably good enrichment on all targets. Some targets give better enrichments using one scoring function, while others perform much better using an alternative scoring function. In particular, for a particular scoring function there is not even a general cutoff value, and for each protein target the best cutoff value needs to be identified. Thus, the score of a putative binder from a library needs to be related to the scores of known binders. To compare the quality of new scoring functions, the enrichment of benchmark datasets such as PDBbind[57,58] or DUD[19] are cal-

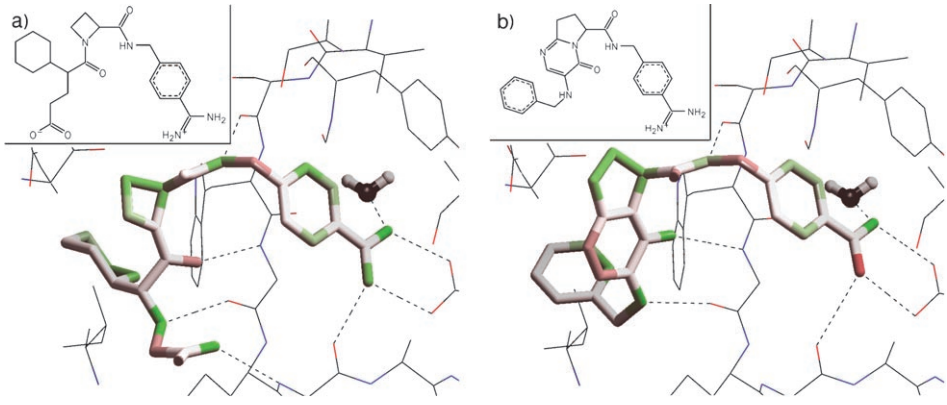

Figure 7. 3D representation of a) thrombin inhibitor 1K22 and b) decoy ZINC03842250 according to the HYDE atom score contributions.

culated. However, Seifert recently showed that commonly used characteristics such as enrichment factors are not sufficient to prove the discriminatory power of a scoring function.[59] However, even if reliable statistical methods are applied, the results depend on too many influences to draw general conclusions. For instance, the larger the validation data sets grow, the higher the risk for biases and errors in the data which had not been detected by the distributors. In addition, one should keep in mind that enrichment calculations reflect the quality of the whole procedure which includes target and library preparation, the placement of the compounds within the binding pocket, and finally the scoring of the protein–ligand interaction. A less-than-optimal procedure in any of the preceding steps to the scoring may give rise to an unsatisfying enrichment, even if the scoring function may have been able to distinguish between good poses of a binder and a "non-binder".

Current scoring functions do not include the dehydration of polar and apolar groups consistently. For instance, the dehydration of apolar atoms that do not face other apolar atoms in the interface is not included in either of the scoring functions mentioned in the introduction. Furthermore, the dehydration of polar atoms that face apolar atoms in the interface is often ignored. These scoring functions focus on pairwise interaction terms. However, according to our view, the hydrophobic effect is not a force that can be described using pairwise potentials. We developed a new scoring function, HYDE, which is a simple function and contains two main terms only: a) the dehydration of the atoms in the protein–ligand interface and b) hydrogen bond energies. According to our theory,[18] the dehydration of apolar atoms in the interface contributes favorably to the overall binding energy and implicitly includes the hydrophobic effect. In contrast, the dehydration of polar atoms contributes a destabilization to the overall binding and can only be overcompensated if this polar atom is involved in a new hydrogen bond with ideal geometry. The calculation of dehydration terms in HYDE is based on $\log P$ increments, the so-called $p\log P$ values, which were extracted from experimental $\log P$ values. Particular care was taken that the sign and magnitude of the $p\log P$ increments are in agreement with the observation that apolar atoms prefer to avoid water, and polar atoms prefer to be in water. To make the calculations consistent, the reversed relationship between the dehydration of water molecules and the hydrogen bond energy between individual water molecules was used to estimate the hydrogen bond energies of polar atoms from their dehydration contribution.[18] Polar and apolar atoms belonging to the ligand or the protein were treated identically with the same algorithms. As a result, the size of the dehydration of polar and apolar atoms, the vacuum hydrogen bond contribution, and the hydrogen bond contributions in aqueous solution agree well with the experimental values.[60,61]

It was also essential that the descriptions of hydrogen bonds reflect their strong directionality, and that small deviations from ideal geometry result in a significant decrease in the hydrogen bond energy. In HYDE, the total score is the sum of small contributions between -12 and $+8\,kJ\,mol^{-1}$, which, taken on their own, are not significantly smaller than the total score. Differences of $6\,kJ\,mol^{-1}$ correspond to one ΔpIC_{50} unit, and an incorrect protonation state can cost up to $20\,kJ\,mol^{-1}$, which corresponds to a ΔpIC_{50} of 3–4. This confirms, as Leach et al.[3] among others have pointed out before, that "the window of affinity" is quite small, and the exchange of a single atom may cause a medium-binding compound to become inactive. Thus, one should be aware that only a categorization in non-binding-, weak-, medium-, and strong-binding inhibitors is sensible and, as we have shown above, is possible using HYDE.

As an additional consequence, a good score requires the correct placement of the correct stereomer, tautomer, or protomer into its target binding site. Any small mistakes such as a incorrect protonation, bad hydrogen bond geometry, or required conformational changes within the protein binding pocket, lead to a significantly lower score. This is illustrated in the examples above. In the case of the estrogen receptor, FlexX has generated sensible poses for the binders and thus HYDE was able to distinguish between the provided binders and either the decoys or compounds selected randomly from an in-house library. HYDE even suggests that some compounds from the decoy data set may represent lead structures and also provides information on how they should be modified in order to increase their binding affinity. In the case of p38 MAP kinase, the case is somewhat more difficult, as some of the provided binders do not bind into the provided allosteric binding site. However, closer analysis showed that HYDE is able to distinguish clearly between: a) compounds that fit into the provided protein pocket and which, taken separately, gave rise to a significant enrichment in the calculations, b) compounds that bind through a specific hydrogen bond network selectively to the ATP binding site and which gave rise to a significant depletion relative to the decoys, and c) compounds that make few or no hydrogen bonds to the protein and are thus less specific and have an enrichment similar to randomly chosen molecules. In the case of thrombin, HYDE has correctly detected that some provided binders do not bind as such, but require either additional zinc ions or interact covalently with the protein. Most interestingly, HYDE had also been able to identify several compounds within the decoy data set that belong to compound classes disclosed as thrombin inhibitors.

Conclusions

Herein we show that HYDE is able to distinguish between "correct poses of binders" and "non-binders". HYDE has an additional advantage in that the absolute score is target independent, and can be used as a general indicator if a predicted pose is correct and/or if the compound is indeed a binder. However, one should keep in mind that for various reasons such as a bad placement, incorrect protein conformation, or unconsidered cofactors, it is quite likely that some binders are missed or have too low a score. Furthermore, a putative binder may fit into one and not in the alternative target protein conformation. Still, it might be better to overlook some compounds and overlook poses instead of spending a significant amount of time on false-positive hits and falsely predicted poses in the downstream analysis of virtual screening hits. A further advant-

age of HYDE is that the contributions of the individual ligand atoms are calculated, which gives directions as to where modification should be made.

In summary, HYDE reflects the experimentally observed binding contributions due to hydrogen bonding and the hydrophobic effect in a very accurate way. In particular, it reflects correctly that small changes within the protein–ligand interface have a significant effect on the binding of inhibitors, which is one of the primary reasons why inhibitor design is so difficult. The current version of HYDE works best for accurately placed ligands in which the ligand pose has been generated using the geometric parameters derived from small-molecule crystallographic data. Future efforts will focus on including a step in the docking procedure in which the geometry of a given pose will be optimized using HYDE as an objective function. Thus, HYDE could be applied to any protein–ligand structure regardless of its origin.

Computational Section

Calculation of weighted solvent accessibility: We approximate the SAS by a recursive tessellation procedure. The van der Waals radius (r_{vdW}) of an atom is augmented by the probe radius (r_{SAS}), and the vertices of an in-lying icosahedron are each tested for accessibility. If the distance between a vertex and the van der Waals surface of a neighboring atom is less than r_{SAS}, this vertex is assumed to be inaccessible for solvent molecules.

For each triangle on the icosahedron surface three cases are considered: 1) if all three vertices are accessible, the corresponding surface patch is assumed to be completely accessible, and its contribution to the SAS is calculated; 2) in the case that all vertices are inaccessible to the solvent, the triangle does not contribute to the SAS; 3) otherwise, if at least one vertex is accessible and at least one vertex is not accessible, three additional vertices in the centers of the triangle edges are calculated. This results in four smaller spherical triangles. The new triangle vertices are recursively tested for accessibility until a break condition is reached. The corresponding surface contribution is considered proportionally to the number of accessible vertices.

The weighted solvent-accessible surface area (WSAS), which we use in the HYDE scoring function is calculated similar to the SAS. The only difference is that for atoms capable of forming interactions, the accessibility is no longer a 'yes-or-no' consideration. The weighted accessibility of a triangle vertex a_j is affected by the angle deviation factor f_{adev}, which is based on the FlexX interaction surfaces (Figure 8). The weighted accessible surface $wsas_j$ of a triangle patch is calculated corresponding to the weighting factors a_{j1}, a_{j2}, and a_{j3} of its vertices:

$$wsas_j = \frac{4\pi\left(r_{SAS} + r_{vdW}^j\right)^2}{20\,4^n}\,\frac{a_{j1} + a_{j2} + a_{j3}}{3} \qquad (13)$$

in which n is the recursion depth. The a_j are zero if the vertex is not accessible to solvent, otherwise they equal the deviation factor f_{adev}. In the case that an atom has more than one interaction surface, we calculate all corresponding f_{adev} and use the maximum value. For hydrophobic atoms, f_{adev} is always 1. Summing up over all smallest triangle patches $wsas_j$ the total weighted accessible surface area of an atom i is:

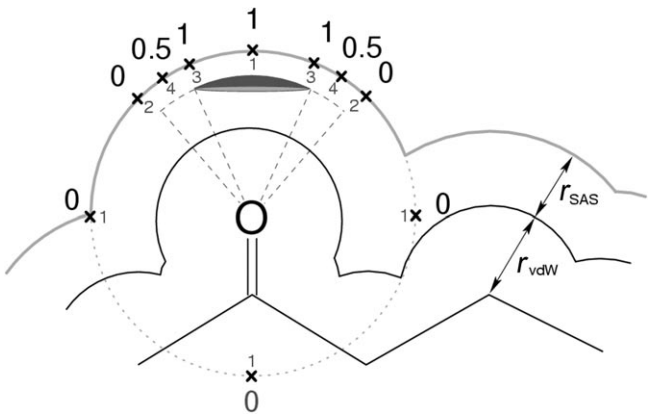

Figure 8. 2D representation of the WSAS tessellation procedure. The smaller numbers inside the dashed circle denote the recursion depth, and the numbers outside, the weighted accessibility of the vertices. Accessibility of hydrophobic atoms is only dependent on the neighboring atoms, while the accessibility of polar atoms is also dependent on the atomic interaction surfaces.

$$WSAS_i = \sum wsas_j \qquad (14)$$

FlexX interaction model: In FlexX the quality of a directed interaction between two atoms is rated regarding the relative orientation of so-called interaction geometries.[30,42] Each interacting group of a molecule is assigned an interaction type and interaction geometry, which is a part of a spherical surface. An interaction between two atoms i and j is identified when the atom interaction types are compatible to each other and the interaction centers lie approximately on the interaction surfaces of the partner atoms (Figure 9). Deviations from ideal geometry are penalized.

$$f_{dev}^{ij} = f_{ldev}(\Delta d_{ij}) f_{adev}(\Delta\alpha_i) f_{adev}(\Delta\alpha_j) \qquad (15)$$

$f_{dev}(i,j)$ is the deviation factor for the specific geometry between i and j. f_{ldev} penalizes deviations Δd from the ideal distance, and f_{adev} penalizes deviations $\Delta\alpha$ from the corresponding angles between i and j. f_{ldev} and f_{adev} equal 1 for a good geometry and decrease linearly with increasing distance and angle, respectively. Some interaction geometries were manually adapted for use within the HYDE scoring function; for example, the hydrogen bond acceptor surface of carbonyl groups was decreased in size in order to better reflect the directionality of such a bond.

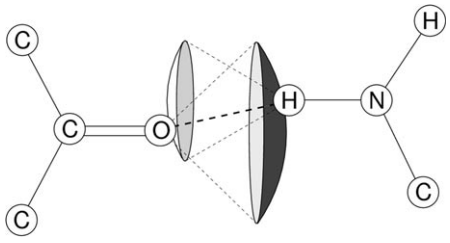

Figure 9. Schematic representation of FlexX interaction surfaces. This hydrogen bond interaction has an ideal geometry, as the interaction centers are positioned on the surfaces of the interacting atoms.

Acknowledgements

The authors thank BioSolveIT GmbH for providing the FlexX software library and many fruitful discussions.

Keywords: computer-aided molecular design · docking · HYDE · scoring functions · virtual screening

[1] H. Kubinyi in *Computer Applications in Pharmaceutical Research and Development* (Ed.: S. Ekins), Wiley, New York, **2006**.
[2] G. L. Warren, C. W. Andrews, A. M. Capelli, B. Clarke, J. LaLonde, M. H. Lambert, M. Lindvall, N. Nevins, S. F. Semus, S. Senger, G. Tedesco, I. D. Wall, J. M. Woolven, C. E. Peishoff, M. S. Head, *J. Med. Chem.* **2006**, *49*, 5912.
[3] A. R. Leach, B. K. Shoichet, C. E. Peishoff, *J. Med. Chem.* **2006**, *49*, 5851.
[4] S. F. Sousa, P. A. Fernandes, M. J. Ramos, *Proteins Struct. Funct. Genet.* **2006**, *65*, 15.
[5] T. Schulz-Gasch, M. Stahl, *Drug Discovery Today* **2004**, *1*, 231.
[6] H. Gohlke, G. Klebe, *Angew. Chem.* **2002**, *114*, 2764; *Angew. Chem. Int. Ed.* **2002**, *41*, 2644.
[7] D. B. Kitchen, H. Decornez, J. R. Furr, J. Bajorath, *Nat. Rev. Drug Discovery* **2004**, *3*, 935.
[8] M. Rarey, J. Degen, I. Reulecke in *Bioinformatics—From Genomes to Therapies, Vol. 2* (Ed.: T. Lengauer), Wiley-VCH, Weinheim, **2007**.
[9] H. J. Savage, C. J. Elliott, C. M. Freeman, J. L. Finney, *J. Chem. Soc. Faraday Trans.* **1993**, *89*, 2609.
[10] P. J. Fleming, G. D. Rose, *Protein Sci.* **2005**, *14*, 1911.
[11] F. Giordanetto, S. Cotesta, C. Catana, J.-Y. Trosset, A. Vulpetti, P. F. W. Stouten, R. T. Kroemer, *J. Chem. Inf. Comput. Sci.* **2004**, *44*, 882.
[12] T. A. Pham, A. N. Jain, *J. Med. Chem.* **2006**, *49*, 5856.
[13] M. D. Eldridge, C. W. Murraz, T. R. Auton, G. V. Paolini, R. P. Mee, *J. Comput.-Aided Mol. Des.* **1997**, *11*, 425.
[14] R. A. Friesner, R. B. Murphy, M. P. Repasky, L. L. Frye, J. R. Greenwood, T. A. Halgren, P. C. Sanschagrin, D. T. Mainz, *J. Med. Chem.* **2006**, *49*, 6177.
[15] A. Krammer, P. D. Kirchhoff, X. Jiang, C. M. Venkatachalam, M. Waldmann, *J. Mol. Graphics Modell.* **2005**, *23*, 395.
[16] G. E. Kellogg, J. C. Burnett, D. J. Abraham, *J. Comput.-Aided Mol. Des.* **2001**, *15*, 381.
[17] R. Wang, L. Lai, S. Wang, *J. Comput.-Aided Mol. Des.* **2002**, *16*, 11.
[18] G. Lange, I. Reulecke, M. Rarey, R. Klein, *ChemPhysChem* **2008**, 10.1002/cphc.200700804.
[19] N. Huang, B. K. Shoichet, J. J. Irwin, *J. Med. Chem.* **2006**, *49*, 6789.
[20] A. K. Soper, *Faraday Discuss.* **1996**, *103*, 41.
[21] P. Broto, G. Moreau, C. Vandycke, *Eur. J. Med. Chem.* **1984**, *19*, 71.
[22] A. K. Ghose, G. M. Crippen, *J. Comput. Chem.* **1986**, *7*, 565.
[23] R. Wang, Y. Gao, L. Lai, *Perspect. Drug Discovery Des.* **2000**, *19*, 47.
[24] T. J. Hou, X. J. Xu, *J. Chem. Inf. Comput. Sci.* **2003**, *43*, 1058.
[25] T. Hou, W. Zhang, Q. Huang, X. Xu, *J. Mol. Model.* **2005**, *11*, 26.
[26] F. M. Richards, *Annu. Rev. Biophys. Biol.* **1977**, *6*, 151.
[27] C. Hansch, A. Leo, D. Hoekman, *Exploring QSAR. Hydrophobic, Electronic, and Steric Constants*, American Chemical Society, Washington DC, **1995**.
[28] http://www.syrres.com/esc/physprop.htm.
[29] E. T. Kool, *Annu. Rev. Biophys. Biomol. Struct.* **2001**, *30*, 1.
[30] H.-J. Böhm, *J. Comput.-Aided Mol. Des.* **1994**, *8*, 243.
[31] G. J. Kleywegt, A. T. Brünger, *Structure* **1996**, *4*, 897.
[32] W. Kabsch, C. Sander, *Biopolymers* **1983**, *22*, 2577–2637.
[33] A. V. Morozov, T. Kortemme, *Adv. Protein Chem.* **2005**, *72*, 1.
[34] C. Pargellis, L. Tong, L. Churchill, P. F. Cirillo, T. Gilmore, A. G. Graham, P. M. Grob, E. R. Hickey, N. Moss, S. Pav, J. Regan, *Nat. Struct. Biol.* **2002**, *9*, 268.
[35] P. Ferrara, H. Gohlke, D. J. Price, G. Klebe, C. L. Brooks III, *J. Med. Chem.* **2004**, *47*, 3032.
[36] R. Wang, Y. Lu, X. Fang, S. Wang, *J. Chem. Inf. Comput. Sci.* **2004**, *44*, 2114.
[37] E. Perola, W. P. Walters, P. S. Charifson, *Proteins Struct. Funct. Genet.* **2004**, *56*, 235.
[38] P. M. Marsden, D. Puvanendrampillai, J. B. O. Mitchell, R. C. Glen, *Org. Biomol. Chem.* **2004**, *2*, 3267.
[39] E. Kellenberger, J. Rodrigo, P. Muller, D. Rognan, *Proteins Struct. Funct. Genet.* **2004**, *57*, 225.
[40] R. S. Pearlman, US 2005125210, **2005**.
[41] S. J. Weiner, P. A. Kollman, D. A. Case, U. C. Singh, C. Ghio, G. Alagona, S. Profeta, Jr., P. Weiner, *J. Am. Chem. Soc.* **1984**, *106*, 765. The augmented force field parameters can be delivered on request.
[42] M. Rarey, B. Kramer, T. Lengauer, G. Klebe, *J. Mol. Biol.* **1996**, *261*, 470.
[43] A. K. Shiau, D. Barstad, J. T. Radek, M. J. Meyers, K. W. Nettles, B. S. Katzenellenbogen, J. A. Katzenellenbogen, D. A. Agard, G. L. Greene, *Nat. Struct. Biol.* **2002**, *9*, 359.
[44] P. Traxler, P. Furet, *Pharmacol. Ther.* **1999**, *82*, 195.
[45] D. J. Diller, R. X. Li, *J. Med. Chem.* **2003**, *46*, 4638.
[46] D. R. Anderson, M. J. Meyers, W. F. Vernier, M. W. Mahoney, R. G. Kurumbail, N. Caspers, G. I. Poda, J. F. Schindler, D. B. Reitz, R. J. Mourey, *J. Med. Chem.* **2007**, *50*, 2647.
[47] T.-S. Kim, J.-C. Harmange, S. Booker, N. D'Angelo, C. Dominguez, I. M. Fellows, L. Liu, A. Tasker, S. Bellon, T. S. Harvey, M. Lee, J. Germain, V. F. Patel, J. L. Kim, US 20070054903, **2007**.
[48] R. Gericke, N. Beier, O. Poeschke, L. Burgdorf, H. Drosdat, F. Lang, WO 2004-EP10398 20040916, **2005**.
[49] R. Krishnan, E. Zhang, K. Hakansson, R. K. Arni, A. Tulinsky, M. S. Lim-Wilby, O. E. Levy, J. E. Semple, T. K. Brunck, *Biochemistry* **1998**, *37*, 12094.
[50] F. Dullweber, M. T. Stubbs, D. Musil, J. Sturzebecher, G. Klebe, *J. Mol. Biol.* **2001**, *313*, 593.
[51] B. A. Katz, J. M. Clark, J. S. Finer-Moore, T. E. Jenkins, C. R. Johnson, M. J. Ross, C. Luong, W. R. Moore, R. M. Stroud, *Nature* **1998**, *391*, 608.
[52] M. M. Chow, E. F. Meyer, W. Bode, C. M. Kam, R. Radhakrishnan, J. Vijayalakshmi, J. C. Powers, *J. Am. Chem. Soc.* **1990**, *112*, 7783.
[53] S. D. Kimball, S. E. Hall, W. F. Lau, EP 623595, **1994**, .
[54] P. W. Glunz, US 2004006065, **2004**.
[55] U. Ries, N. Hauel, G. P. Mihm, H. , K. Binder, J. M. Stassen, W. Wienen, R. Zimmermann, WO 9940072, **1999**.
[56] F. S. Tjoeng, M. V. Toth, WO 9420457, **1994**.
[57] R. Wang, X. Fang, Y. Lu, S. Wang, *J. Med. Chem.* **2004**, *47*, 2977.
[58] R. Wang, X. Fang, Y. Lu, C. Y. Yang, S. Wang, *J. Med. Chem.* **2005**, *48*, 4111.
[59] M. H. Seifert, *J. Chem. Inf. Model.* **2006**, *46*, 1456.
[60] A. R. Fersht, J. P. Shi, J. Knilljones, D. M. Lowe, A. J. Wilkinson, D. M. Blow, P. Brick, P. Carter, M. M. Y. Waye, G. Winter, *Nature* **1985**, *314*, 235.
[61] G. A. Jeffrey, *An Introduction to Hydrogen Bonding*, Oxford University Press, Oxford, UK, **1997**.
[62] Z. Wang, B. J. Canagarajah, J. C. Boehm, S. Kassisa, M. H. Cobb, P. R. Young, S. Abdel-Meguid, J. L. Adams, E. J. Goldsmith, *Structure* **1998**, *6*, 1117.

Received: November 8, 2007
Revised: February 25, 2008
Published online on April 2, 2008

